

Discovery of a bipolar and highly variable mass outflow from the symbiotic binary StH α 190*

U. Munari^{1,2}, T. Tomov^{2,3}, B. F. Yudin⁴, P. M. Marrese^{1,2}, T. Zwitter⁵, R. G. Gratton⁶, G. Bonanno⁷, P. Bruno⁷, A. Calí⁷, R. U. Claudi⁶, R. Cosentino^{7,8}, S. Desidera⁶, G. Farisato⁶, G. Martorana¹, G. Marino⁸, M. Rebeschini¹, S. Scuderi⁷, and M. C. Timpanaro⁷

¹ Osservatorio Astronomico di Padova, Sede di Asiago, 36032 Asiago (VI), Italy

² Center of Studies and Activities for Space (CISAS “G. Colombo”), University of Padova, Italy

³ Center for Astronomy, Nicolaus Copernicus University, ul. Gagarina 11, 87100 Torun, Poland

⁴ Sternberg Astronomical Institute, Universitetskii pr. 13, Moscow 119899, Russia

⁵ Department of Physics, Univ. of Ljubljana, Jadranska 19, 1000 Ljubljana, Slovenia

⁶ Osservatorio Astronomico di Padova, Vicolo dell’Osservatorio 5, 35122 Padova, Italy

⁷ Osservatorio Astrofisico di Catania, Via S. Sofia 78, 95123 Catania, Italy

⁸ Centro Galileo Galilei – CNAA, Calle Alvarez de Abreu 70, 38700 Santa Cruz de La Palma (TF), Spain

Received 26 January 2001 / Accepted 6 February 2001

Abstract. A highly and rapidly variable bipolar mass outflow from StH α 190 has been discovered, the first time in a yellow symbiotic star. Permitted emission lines are flanked by symmetrical jet features and multi-component P-Cyg profiles, with velocities up to 300 km s⁻¹. Given the high orbital inclination of the binary, if the jets leave the system nearly perpendicular to the orbital plane, the de-projected velocity equals or exceeds the escape velocity (1000 km s⁻¹). StH α 190 looks quite peculiar in many other respects: the hot component is an O-type sub-dwarf without an accretion disk or a veiling nebular continuum and the cool component is a G7 III star rotating at a spectacular 105 km s⁻¹, unseen by a large margin in field G giants.

Key words. binaries: symbiotic – stars: individual: StH α 190 – interstellar medium: jets and outflows

1. Introduction

StH α 190 has been independently discovered on objective prism plates by Kinman (1983, private communication to Whitelock et al. 1995, hereafter W95) and Stephenson (1986). Its symbiotic nature was noted during the spectroscopic survey of StH α objects by Downes & Keyes (1988). The 3300–9100 Å absolutely fluxed spectrum of StH α 190 included in the spectrophotometric atlas of 137 symbiotic stars by Munari & Zwitter (2001, hereafter MZ01) shows a well developed G-type continuum with minimal veiling by the nebular or hot companion continua and a pronounced emission line spectrum of moderate excitation (HeII missing) with strong [OIII] and [NeIII] forbidden lines. Minimal – if any – changes arise in the comparison with older available spectroscopy. The IUE spectrum of StH α 190 by Schmidt & Nussbaumer (1993, hereafter SN93) confirms the moderate excitation conditions (NV

and HeII missing) and shows the photospheric continuum of an O sub-dwarf without contribution from nebular regions or an accretion disk.

Data from the Munari et al. (2001, hereafter MHZ) *UBV(RI)_C* photometric survey of symbiotic stars confirms a rather limited variability of StH α 190 and absence of outbursts since its discovery, reporting $V = 10.50$, $(B - V) = +0.84$, $(U - B) = -0.23$, $(V - R)_C = +0.50$ and $(V - I)_C = +0.47$ for mid 2000. W95 infrared photometry of StH α 190 over 16 nights from Oct. 1983 to Jul. 1987 gives $K = 7.81$, $J - H = +0.57$, $H - K = +0.36$ and $K - L = +0.95$ as mean values. In *J* and *H* bands W95 did not find evidence of variability while a modest $\Delta K = 0.16$ is attributed to changes in the heating of the circumstellar dust by the hot source.

In this *Letter* we report about the discovery of highly variable bipolar mass outflow and blob ejection from StH α 190, the first time in a *yellow* symbiotic star. Yellow SS harbour warm giants (F, G or early K type), which have much smaller dimensions and lower mass loss rates compared to the M giants of classical symbiotics. Jets and bipolar outflows have been so far discovered in only five other symbiotic stars (among the ~225 known), all of

Send offprint requests to: U. Munari,
e-mail: ulisse@ulisse.pd.astro.it

* Based in part on observations secured with SARG at Telescopio Nazionale Galileo (TNG), La Palma, Canary Islands.

Table 1. Journal of spectroscopic observations and measured radial velocities. *A* = Asiago Echelle+CCD spectrograph operating at $R = 18\,500$ resolving power, *S* = the SARG Echelle+CCD spectrograph at $R = 57\,000$. The heliocentric radial velocities of HeI 5876 and [OIII] 4959 Å pertain to the main emission component, those of NaI to the stellar 5890–5896 doublet de-blended from the interstellar components. Data on H α includes heliocentric radial velocities of the main component (*mc*), the blue shifted jet (*b_J*) and the red shifted jet (*r_J*), as well as the component widths corrected for the instrumental PSF

Date	UT		RV _⊙ (km sec ⁻¹)						FWHM (km sec ⁻¹)		
			NaI	HeI	[OIII]	H α			H α		
						<i>mc</i>	<i>b_J</i>	<i>r_J</i>	<i>mc</i>	<i>b_J</i>	<i>r_J</i>
Aug 14	24:22	A	5.4	15.8	18.2	13.8	-116	154	48	185	120
Aug 16	23:45	A	19.0	14.9	17.9	13.8	-123	158	43	125	150
Sep 09	22:20	A	-2.1	18.3	19.4	16.1	-82	134	44	230	280
Sep 10	23:35	A	12.6	17.8	19.1	15.1	-85	137	45	205	245
Sep 11	24:35	A	13.7	17.8	19.6	15.0	-87	132	46	210	215
Oct 09	21:19	S	-17.4	14.1	14.4	14.4	-97	103	42	190	250
Oct 10	20:47	S	-14.9	15.5	14.3	14.1	-88	106	42	200	245
Nov 04	24:14	S	-5.2	17.9	18.0	16.5	-55	102	42	185	215
Nov 05	20:44	S	-4.5	18.1	18.1	17.2	-66	147	42	190	200
Nov 06	21:41	S	-5.2				-68	93	42	170	190
Nov 07	22:49	S	-5.6	18.7	18.3	17.6	-70	77	42	210	225
Dec 15	17:19	A	16.4	18.2	16.3	-71	113	44	305	240	
Dec 17	16:58	A	-18.7	16.4	17.4	15.4	-66	106	47	235	210
			<i>mean value</i>	16.8	17.7	15.4					
				± 0.4	± 0.4	± 0.5					

them containing M giants or Miras and showing outburst activity: R Aqr (Burgarella & Paresce 1992), CH Cyg (Taylor et al. 1986), MWC 560 (Tomov et al. 1990), RS Oph (Taylor et al. 1989) and Hen 3-1341 (Tomov et al. 2000).

2. Observations

$R = \frac{\lambda}{\Delta\lambda} = 18\,500$ spectra have been obtained with the Echelle spectrograph mounted at the Cassegrain focus of the 1.82m telescope which is operated by the Padova and Asiago Astronomical Observatories on top of Mt. Ekar (Asiago, Italy). The detector has been a Thomson THX31156 CCD with 1024×1024 pixels, 19 μ m each, and the slit width has been set to 1.8 arcsec. The spectra cover the 4500–9000 Å range.

$R = \frac{\lambda}{\Delta\lambda} = 57\,000$ spectra have been obtained during the commissioning phase of the SARG white-pupil Echelle spectrograph for the Italian 3.5 m Telescopio Nazionale Galileo (La Palma, Canary Islands). The detector is a mosaic of two 4k × 2k thinned, back illuminated EEV CCDs. A 0.80 arcsec slit width has been used together with the YELLOW cross-disperser grism which provides a nearly complete spectral coverage from 4650 to 7900 Å. A journal of the observations is given in Table 1.

Infrared photometry has been obtained at the 1.25 m telescope of the Crimean Astrophysical Observatory, giving $J = 8.74$, $H = 8.25$, $K = 8.08$, $L = 7.48$ on Nov. 20 and $J = 8.74$, $H = 8.22$, $K = 8.04$, $L = 7.52$ on Dec. 8, 2000 (with errors ± 0.02 in JHK , ± 0.04 in L).

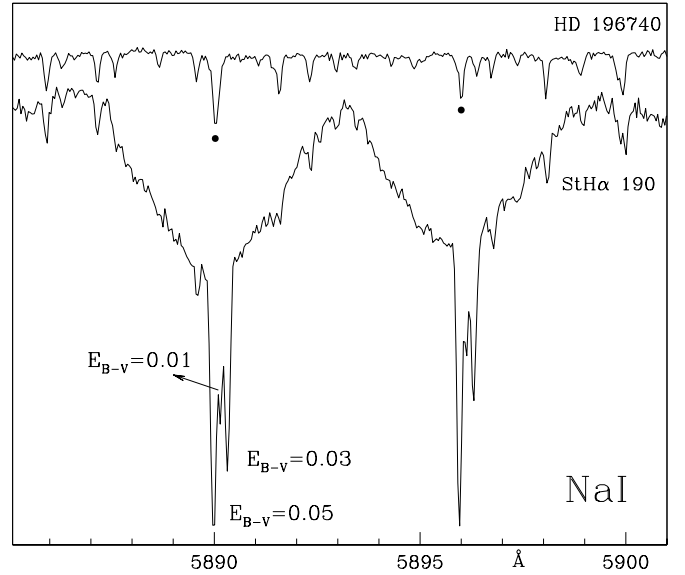


Fig. 1. The region around the NaI doublet, showing the rotationally broadened stellar component and three sharper interstellar lines (SARG spectrum for Oct. 9, 2000). The upper spectrum shows the telluric absorptions in 28 Vul, a B6 IV fast rotating star ($V_{\text{rot}} \sin i = 320 \text{ km s}^{-1}$) observed on the same night as StH α 190. 28 Vul suffers from a $E_{B-V} \sim 0.01$ responsible for the interstellar NaI lines marked by dots. Comparing 28 Vul and StH α 190 spectra reveals how nearly all the sharp and weak lines in the latter spectrum are telluric

3. System properties

3.1. Classification, distance, interstellar lines and reddening

The 3300–9100 Å spectra of StH α 190 and MKK standards in MZ01 allows us to classify the cool giant as G7 III. Comparing MHZ photometry with the intrinsic colours from Fitzgerald (1970) and absolute magnitudes from Schmidt-Kaler (1982), the reddening turns out to be $E_{B-V} = 0.10$ and the distance $d = 575 \text{ pc}$. SN93 estimated an identical $E_{B-V} = 0.10$ from the 2175 Å interstellar hump in the IUE spectra of StH α 190.

Multiple interstellar components are superposed on the rotationally broadened stellar NaI doublet (cf. Fig. 1). Their RV_{\odot} are $-18.1 (\pm 0.5)$, $-10.0 (\pm 0.5)$ and $-0.9 (\pm 0.4) \text{ km s}^{-1}$, with 0.159, 0.051 and 0.112 (± 0.003) Å as equivalent widths for the 5889 component, respectively. They are unresolved on the Asiago spectra and the blend has $RV_{\odot} = -10.8 (\pm 0.5) \text{ km s}^{-1}$. StH α 190 is at $b = -36^\circ$ so our line-of-sight exits the galactic dust layer (assumed to reach $\Delta z \sim 100 \text{ pc}$ over the galactic plane) at the projected distance of $\sim 170 \text{ pc}$, where the effect of the galactic rotation on the radial velocity does not exceed 2 km s^{-1} . None of the three interstellar lines shares the velocity of the StH α 190 circumstellar material (see bottom line in Table 1), so they have to originate in distinct clouds with RV dispersion similar to that of extreme Pop I objects (12.5 km s^{-1} , Binney & Merrifield 1998). If we use the NaI vs. E_{B-V} calibration of Munari & Zwitter (1997), the equivalent widths of the three

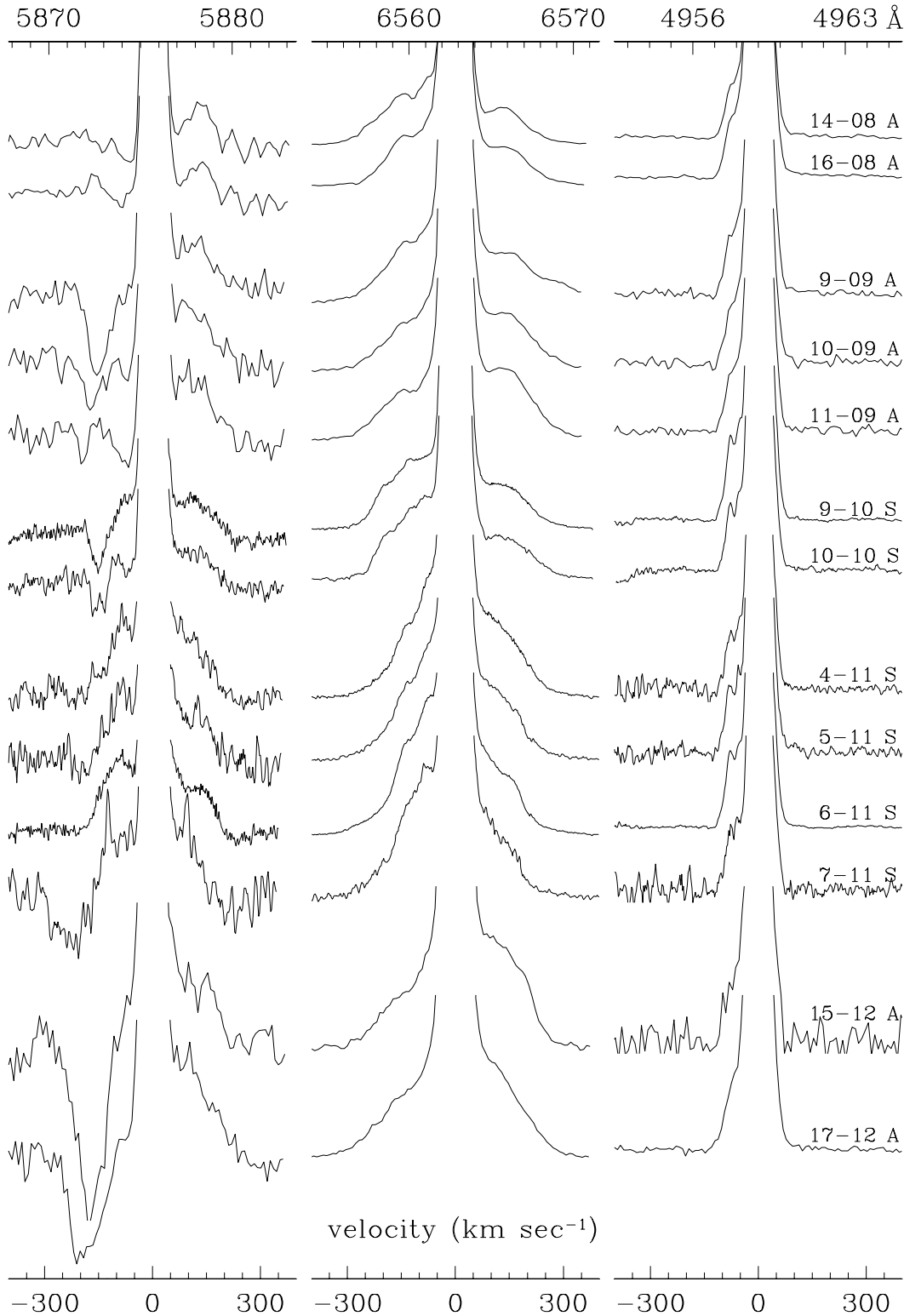


Fig. 2. Evolution of the HeI, H α and [OIII] emission line profiles over a 4 month period (see dates on the right and Table 1); *S* = SARG, *A* = Asiago spectra. The higher resolution of SARG spectra is the reason for the *apparent* variability of the [OIII] line, which is actually pretty constant. The vertical scale is constant for each line (expansion factors 1:7.2:7.2), the continuum is normalised and the line profiles are truncated

interstellar NaI components correspond to $E_{B-V} = 0.049$, 0.016 and 0.035, respectively, giving a total $E_{B-V} = 0.10$, a value identical to what above derived by independent methods.

3.2. Radial velocities and orbital motion

Heliocentric velocities of the main emission lines and the stellar NaI absorption which traces the G7 III star are listed in Table 1. The fairly constant RV_{\odot} of emission

lines indicates that their formation regions do not follow the orbital motion and are circumstellar in origin.

The stellar NaI doublet clearly shows orbital motion velocity shifts, even if the observations did not cover a full orbital cycle. Lower limit to the velocity amplitude ($\Delta RV_{\odot} \sim 30 \text{ km s}^{-1}$) is remarkable for a symbiotic star and it is the largest recorded so far (see Table 4 of Belczyński et al. 2000). This suggests a large orbital inclination, an unusually massive hot companion and a short orbital period.

3.3. Photometric variability

StH α 190 has been detected by Tycho at the limit of its sensitivity range during 78 passages distributed over 17 dates (from Dec. 27, 1989 to Dec. 14, 1992). Automatic analysis of Tycho data summarized in the Hipparcos Catalogue did not detect variability of StH α 190 over the large noise in the B_T and V_T data. Our recent IR photometry reported in Sect. 2 is in excellent agreement with the older W95 data.

However, if a detailed search for variability and periodicities is performed on Tycho and W95 data as well as on the radial velocities of Table 1, an average periodicity of 171 ± 5 days (and its 115 ± 7 yearly alias) is found. If this corresponds to the orbital period it would be the shortest known among all symbiotic stars, followed by those of two other yellow symbiotics TX CVn (199 days) and BD-21.3873 (282 days) and the recurrent symbiotic nova T CrB (228 days; cf. Belczyński et al. 2000 and references therein).

3.4. Rotational velocity

The width of the stellar NaI absorption lines in Fig. 1 corresponds to $V_{\text{rot}} \sin i \sim 105 \text{ km s}^{-1}$, which translates into a 5 days rotation period for the G7 III star, much less than the possible 171 day orbital period. Such a rotational velocity is very high: from the catalogue of rotational velocities of Bernacca & Perinotto (1973) the mean value for the 288 giants between G2 K2 is $V_{\text{rot}} = 9.7 \text{ km s}^{-1}$, with 92% of them having $V_{\text{rot}} \leq 10 \text{ km s}^{-1}$. The high $V_{\text{rot}} \sin i$ further strengthens the idea of a high orbital inclination for StH α 190.

4. The bipolar jets and blobby mass outflow

Figure 2 presents the temporal evolution of HeI 5876 Å emission line profile as a template for other helium lines, H α for hydrogen, and [OIII] for the nebular lines. Over the observational period no other substantial change affected the spectrum of StH α 190.

The H α profile is dominated by a central component that has remained remarkably constant over the last four mounts (see Table 1). Two weaker and symmetrically placed components are flanking the central component. They show large day-to-day variability in both RV_{\odot} and width (cf. Table 1). We identify them as spectral signatures of jet-like discrete ejection events. Weak P-Cyg absorptions interfere with the blue jet component,

reducing its width and its velocity shift vs. the main H α component. Orbital inclination of StH α 190 is probably high, so the de-projected velocity of the jet components must be much larger than the observed velocity shifts ($\sim 150 \text{ km s}^{-1}$) and well in excess of the escape velocity from the O sub-dwarf companion to the G7 III ($\sim 1000 \text{ km s}^{-1}$). The mass of the gas originating the jets is $10^{-11} M_{\odot}$, while the circumstellar ionized region has $M = 1 \cdot 10^{-6} M_{\odot}$ and $R = 4.5 \cdot 10^{14} \text{ cm} = 30 \text{ AU}$ (assuming a simple spherically symmetric geometry). The mass loss rate necessary to sustain the jets is $\dot{M} \sim 5 \cdot 10^{-8} (V_{\text{jet}}/1000 \text{ km s}^{-1}) M_{\odot} \text{ yr}^{-1}$.

The jet components are visible in the profiles of HeI lines too (see HeI 5876 Å in Fig. 2). The velocity and profile of the red component corresponds closely to that seen in the H α profile. The most outstanding feature of the HeI profile is however the multi-component and highly variable P-Cyg component, with terminal velocity even in excess of 300 km s^{-1} . The P-Cyg absorption can be so strong as to completely overwhelm the jet's blue component. The P-Cyg profiles evolve on a few days or hours time scale. The strong P-Cyg component on Sep. 9 (see Fig. 2), for example, accelerated outward by $20 \text{ km s}^{-1} \text{ day}^{-1}$ and dissolved in the next two days, while being replaced by a growing and accelerating new P-Cyg component. The typical mass involved in the absorption profiles is $M = 10^{-11} - 10^{-10} M_{\odot}$.

The relative appearance of hydrogen and HeI lines in StH α 190 closely resembles Hen 3-1341 and its well developed jets and mass outflow (Tomov et al. 2000). We are continuing with the photometric and spectroscopic monitoring and a detailed modeling of StH α 190 will be presented elsewhere.

References

- Belczyński, K., Mikolajewska, J., Munari, U., Ivison, R. J., & Friedjung, M. 2000, A&AS, 146, 407
- Bernacca, P. L., & Perinotto, M. 1973, A Catalogue of Stellar Rotational Velocities (Cleup press, Padova)
- Binney, J., & Merrifield, M. 1998, Galactic Astronomy (Princeton U Press)
- Burgarella, D., & Paresce, F. 1992, ApJ, 389, L29
- Downes, R. A., & Keyes, C. D. 1988, AJ, 96, 777
- Fitzgerald, M. P. 1970, A&A, 4, 234
- Munari, U., & Zwitter, T. 2001, A&A, submitted
- Munari, U., Henden, A., & Zwitter, T. 2001, A&A, to be submitted
- Munari, U., & Zwitter, T. 1997, A&A, 318, 269
- Schmid, H. M., & Nussbaumer, H. 1993, A&A, 268, 159
- Schmidt-Kaler, Th. 1982, in Landolt-Bornstein Series, vol. 2 Astron. Astrophys. (Springer-Verlag, Berlin)
- Stephenson, C. B. 1986, ApJ, 300, 779
- Taylor, A. R., Seaquist, E. R., & Mattei, J. A. 1986, Nature, 319, 38
- Taylor, A. R., Davis, R. J., Porcas, R. W., et al. 1989, MNRAS, 237, 81
- Tomov, T., Kolev, D., Zamanov, R., & Antov, A. 1990, Nature, 346, 637
- Tomov, T., Munari, U., & Marrese, P. M. 2000, A&A, 354, L25
- Whitelock, P. A., Menzies, J., Feast, M. W., et al. 1995, MNRAS, 276, 219